Sensors & Actuators: B. Chemical 297 (2019) 126781

Contents lists available at ScienceDirect

Sensors and Actuators B: Chemical

journal homepage: www.elsevier.com/locate/snb

Lowering the limit of detection of ion-selective membranes backside contacted with a film of poly(3-octylthiophene)

Kequan Xu, Maria Cuartero*, Gaston A. Crespo*

Department of Chemistry, School of Engineering Science in Chemistry, Biotechnology and Health, KTH Royal Institute of Technology, Teknikringen 30, SE-100 44, Stockholm, Sweden

ARTICLE INFO

Keywords:
Thin voltammetry membranes
Poly(3-octylthiophene)
Silver ionophore
Nanomolar silver
Natural and environmental waters

ABSTRACT

Nanometer-sized membranes (thickness of ca 200 nm) backside contacted with a film of poly(3-octylthiophene) (POT) are here interrogated by an electrochemical protocol based on the accumulation and stripping of the target ion aiming at lowering its limit of detection (i.e., in the sub-micromolar range). Thus, using a membrane based on silver ionophore IV (Sigma-Aldrich), which is one of the ionophores regularly used in ion-selective membranes presenting a large binding constant (log $\beta_{Ag-ionophore} \approx 12$), it is possible to detect 5 nM concentration of silver with the established methodology. Importantly, this is a 1000-fold lower concentration of silver compared with the case in which the same membrane is subjected to traditional cyclic voltammetry. Essentially, the control of the oxidation state of the POT film by applying a constant potential during a certain period of time (i.e., $E_{app} = 0$ V for 720 s) in the presence of silver ions in the sample solution (from 5 to 100 nM) allows for an enrichment of the selective membrane in silver ions. As a result, a subsequent anodic linear sweep potential generates a voltammetric peak for silver transfer across the membrane that comprises a well-defined wave for such very low concentrations of silver in high sodium ion concentration background solution (10 mM $NaNO_3$). Detection of nanomolar levels of silver in different types of natural and environmental waters is herein demonstrated and the results are validated using inductively coupled plasma mass spectrometry.

1. Introduction

Polymeric membranes comprising selective receptors (traditionally termed as ionophores) and with a thickness of hundreds of micrometers (ca 300 µm) are the core of potentiometric ion-selective electrodes (ISEs) [1]. Despite potentiometric ISEs currently operating in many different scenarios, e.g., from clinical analyzers to environmental sensors [2], the way in which ion fluxes across the utilized membranes is conceived has evolved over the last decade, mainly with a threefold purpose: (i) the provision of calibration-free sensors, (ii) the improvement of the limit of detection of the ISEs, and (iii) the detection of multiple analytes using only one electrode. As a result, different strategies are daily proposed in the literature following the direction of using a dynamic electrochemical technique to modulate the ion-transfer process across ion-selective membranes (ISMs) rather than its interrogation at zero current [3].

In the direction of providing calibration-free sensors, the most successful approaches are based on thin-layer samples (thickness of ~100 µm) confined in the immediate vicinity of the ISM [4]. Whether an external electrical perturbation (i.e., constant or linear sweep potential) is applied to the system, an exhaustive ion-transfer process is imposed in the entire thin-layer sample. Consequently, the charge associated with this transfer, mainly involving the target ion, is proportional to its concentration in the sample and this is the heart of the calibration-free approach [5].

It is worth mentioning that important advances comprising the dynamic control of ion-transfer processes across ISMs have been simultaneously developed for the all-solid-state concept of the ISEs [6]. Thus, the presence of redox-active films, such as conducting polymers, at the buried interface of the ISM allows for the tuning of any ion transport at the membrane|sample interface in ISMs with reduced thicknesses. In this sense, Amemiya et al. developed a series of electrodes based on a double-layer design comprising a film of doped poly (3,4-ethylenedioxythiophene), or PEDOT-C_{14}, and 1-µm-thick ISM containing the corresponding ionophore for the selective detection of either potassium [7], ammonium [7], or calcium [8], together with the lipophilic salt tetradodecylammonium tetrakis(pentafluorophenylborate) ($TDDA^+TFAB^-$). By using this configuration, the membrane is enriched with the target, this process being triggered by the reduction of the doped PEDOT-C_{14} to its neutral form over the

* Corresponding authors.
E-mail addresses: mariacb@kth.se (M. Cuartero), gacp@kth.se (G.A. Crespo).

https://doi.org/10.1016/j.snb.2019.126781
Received 6 May 2019; Received in revised form 20 June 2019; Accepted 4 July 2019
Available online 05 July 2019

application of a constant potential. Afterward, the linear sweep stripping of the target is coupled to the re-oxidation process of the PEDOT-C_{14} through doping with the $TFAB^-$ present in the membrane.

Following this procedure, the authors demonstrated nanomolar detection of potassium and ammonium in ultrapure water and laboratory-purified water [7], as well as calcium in the same kind of samples [8]. Unfortunately, this elegant concept was not further developed toward the analysis of real and more complex samples. Indeed, when the electrode is interrogated using regular cyclic voltammetry (at a micromolar concentration of the targeted cation) the voltammograms displayed irreversible peaks (i.e., no peak in the anodic scan, or relatively small compared with the cathodic one). This suggests somehow that the PEDOT-C_{14} oxidation/reduction is not entirely reversible in such particular doping conditions. Besides, this behavior may affect the lifetime of the sensor, and probably limits the analytical horizons of the methodology.

Despite other electroactive species also being used to modulate ion-transfer processes in a similar manner as the PEDOT-C_{14}—we are referring to 7,7,8,8-tetraquinodimethane or tetrathiafulvalene [9,10], as well as ferrocene, osmium, and helicene derivatives directly dissolved in the membrane [11–15]—none of these approaches has yet reached the unique analytical performances demonstrated for nanometer-sized membranes (ca 230 nm thickness) backside contacted with a film of the conducting polymer poly(3-octylthiophene), dubbed POT. The differences between this latter system and that reported by Amemiya et al. are: the thickness of the membrane, the incorporation of the cation-exchanger sodium tetrakis[3,5-bis(trifluoromethyl)phenyl]borate (Na^+TFPB^-) instead of $TDDA^+TFAB^-$ and the use of neutral POT rather than doped PEDOT-C_{14} in the initial state of the double-layer electrode. Thus, the displayed voltammetric peaks for the cation transfer are totally reversible and with a Gaussian-based shape [16,17], in contrast to those reported for the PEDOT-based electrode [7,8]. The working mechanism is based on the oxidation of POT to POT^+, this latter being paired with the $TFPB^-$ present in the membrane, and therefore, causing the release of Na^+ to the solution. This mechanism based on the doping of POT^+ exclusively by $TFPB^-$ was largely demonstrated by 'control' electrochemical experiments as well as theoretically modelled [17–19].

Advantageously, thin membranes comprising NaTFPB are compatible with the incorporation of any cation ionophore. Specifically, in the case of the silver ionophore IV (Sigma-Aldrich), it was demonstrated that the membrane may operate under two different regimes according to the amount of the target in the solution. For example, under mass-transport diffusional conditions (the peak height current increases with the cation concentration, i.e., amperometric response-mode), or following a thin-layer behavior (the peak potential shifts to more positive potentials with the cation concentration, i.e., potentiometric response) [18]. Another unique feature of this type of membrane comprises the simultaneous incorporation of several ionophores (up to three) when the membrane operates in a thin-layer regime (i.e., negligible mass-transport limitation either in the membrane or the solution). This allows for the simultaneous detection of multiple cations even in such a complex matrix as undiluted human blood [20,21].

In the present paper, we demonstrate for the first time the interrogation of nanometer-sized ISMs (ca 200 nm) backside contacted with POT with an accumulation/stripping electrochemical protocol aimed at lowering the limit of detection traditionally displayed by this type of membrane. For example, in the case of a silver-selective membrane (based on silver ionophore IV, Sigma-Aldrich), the limit of detection was ca 1 μM under diffusion-controlled response and 50 μM under the thin-layer regime [18]. The principle proposed herein is, in some way, analogous to the stripping voltammetry traditionally applied with the mercury electrode: the preconcentration of the analyte occurs under convective conditions over a certain period of time followed by anodic stripping voltammetry. However, the main difference is that the accumulation of the target occurs at a certain applied potential to control the oxidation state of the POT film while the targeted cation (Ag^+ in our case) is being accumulated in the membrane. Then, there is no redox reaction of the analyte, but instead, there is a cation transfer across the membrane|sample interface during the anodic stripping voltammetry step, which is expected to be enhanced owing to the previous accumulation of silver ions in the ISM. The proposed change in the *modus operandi* of nanometer-sized voltammetry ISMs in combination with a deep exploration of all the experimental parameters influencing the cation (Ag^+) transfer at the membrane|sample interface may lead to a new wave of sensors with an improved limit of detection in the near future.

2. Materials and methods

2.1. Reagents, materials, and equipment

Aqueous solutions were prepared by dissolving the appropriate salts in deionized water (18.2 MΩ·cm). Lithium perchlorate (> 98%, $LiClO_4$), 3-octylthiophene (97%), silver nitrate ($AgNO_3$), sodium nitrate ($NaNO_3$), high-molecular-weight poly(vinyl chloride) (PVC), bis(2-ethylhexyl)sebacate (DOS), sodium tetrakis[3,5-bis(trifluoromethyl) phenyl]borate (NaTFPB), silver ionophore IV, acetonitrile (ACN), and tetrahydrofuran (> 99.9%, THF) were purchased from Sigma-Aldrich and used as received.

Glassy carbon GC-electrode tips (Model 6.1204.300) with an electrode diameter of 3.00 ± 0.05 mm were sourced from Metrohm (Sweden). Cyclic voltammograms were recorded with a PGSTAT128 N (Metrohm Autolab B.V., Utrecht, The Netherlands) controlled by Nova 2.0 software (supplied by Autolab) running on a personal computer. A double junction Ag/AgCl/3 M KCl/1 M LiOAc reference electrode (Model 6.0726.100, Metrohm, Switzerland) and a platinum electrode (Model 6.0331.010, Metrohm, Switzerland) were used in a three-electrode cell. A rotating disk electrode (Model EDI 101, LANGE, Switzerland) was used to spin coat the membranes on the electrodes at 1500 rpm.

2.2. Preparation of the electrodes

Poly(3-octylthiophene) (POT) was electrochemically polymerized on a GC electrode using cyclic voltammetry (two scans, 0–1.5 V, 100 $mV{\cdot}s^{-1}$) and then discharged at 0 V for 120 s, as reported elsewhere [17]. A solution containing 0.1 M 3-octylthiophene and 0.1 M $LiClO_4$ in ACN was used for this purpose. N_2 was purged into the solution for 30 min before use. After the electropolymerization of POT, the electrode was immersed in pure ACN for 30 min and 30 s in THF, and then quickly dried with N_2. The absence of ClO_4^- ion in the POT layer lattice or surface was confirmed in our previous studies using synchrotron-based radiation measurements [19].

Thereafter, a volume of 25 μL of diluted membrane cocktail (50 μL of silver membrane cocktail + 250 μL THF) was spin-coated on the top of the POT-based electrode. The composition of the silver membrane cocktail was 30 wt% of PVC, 60 wt% of DOS, 40 mmol kg^{-1} of NaTFPB, and 80 mmol kg^{-1} of silver ionophore IV, as previously reported [18]. More specifically, approx. 30 mg of PVC, 60 mg of DOS, 3.5 mg of NaTFPB and 6.5 mg of silver ionophore IV were dissolved in 1 ml of THF and then this cocktail was diluted as above detailed.

2.3. Determination of silver in real samples

All the containers used through this paper, including beakers, bottles, and falcon tubes, were of plastic nature and were washed as follows: all the materials were immersed in 10 vv% HNO_3 for 1 day and then thoroughly washed with abundant MilliQ (MQ) water.

The tap water was sampled from the tap water line in the laboratory and was stored in the fridge at 4 °C. The lake water was sampled from Laduviken Lake in Stockholm, Sweden. Both types of samples were analyzed without any pretreatment using the developed electrodes. In

the case of the inductively coupled plasma mass spectrometry (ICP-MS) analysis, the tap and lake waters were first extensively filtered through regular filter paper (a 150 mm Ø, Whatman™) twice, to eliminate all the bigger supernatant particles, and then through 0.45 µm pore-size filters coupled to syringes. In addition, samples spiked with known amounts of Ag^+ were prepared in 1 vv% HNO_3 media.

3. Results and discussion

As recently demonstrated, thin voltammetry membranes comprising Ag ionophore may operate under two different regimes according to the Ag^+ concentration present in the bulk sample solution [18]. At approximately 50 µM Ag^+ concentration, there is a transition from the sole voltammetric peak displayed in the background electrolyte ($NaNO_3$), which corresponds to Na^+ transfer across the membrane, to a single peak associated with the ionophore-assisted Ag^+ transfer across the membrane. As a result, the current of the Na^+ peak decreases whereas the Ag^+ one increases. Note that the total amount of charge transferred across the membrane (i.e., the sum of the integrated charge under the Na^+ and Ag^+ peaks) remained constant over the experiment. On the other hand, when the peak attributed to the Ag^+ remains invariable in terms of peak current, it shifts to more positive values for increasing Ag^+ concentration in the solution, indicating the transition between the two operating modes [18]. In both situations, the exchange process occurring at the membrane-sample interface was theoretically defined by a Nernst-type equation for silver and sodium strictly based on their activities [18]. In the present paper, we propose to interrogate nanometer-sized membranes based on the Ag ionophore under accumulation/stripping electrochemical protocol (diffusion-control mode) rather than regular cyclic voltammetry, to lower the Ag^+ detection to nanomolar levels.

3.1. Nanometer-sized membrane based on silver ionophore interrogated by accumulation/stripping electrochemical protocol

Fig. 1 illustrates the working mechanism of the membrane subjected to the accumulation/stripping electrochemical protocol together with the expected trends for the stripping voltammetric peaks. Essentially, the strategy is based on two steps: 1) the application of a constant potential to assure that POT is mainly in its neutral form, which results in the accumulation of silver ion into the membrane by diffusional mass transport, and 2) the measure of any cation existing in the membrane by using an anodic linear sweep potential as detailed in the following:

Case 1. Only the background electrolyte is present in the sample solution: In the presence of 10 mM $NaNO_3$ (Fig. 1a) only one stripping peak corresponding to Na^+ transfer is expected. Thus, during the application of a constant potential, for example –0.23 V with respect to the open circuit potential (OCP) (i.e., E_{app} = 0 V), at which POT is supposed to be entirely in its neutral form as demonstrated in our previous studies [19], the entrance of Na^+ from the solution may occur to pair $TFPB^-$ (also labeled as R^-) as a consequence of the reduction of any possible POT^+ initially present in the membrane. Although the most stable form of POT is the neutral one, it is also possible that some traces of POT^+ are present when no potential is applied to the electrode, i.e., at OCP conditions [19]. The application of a constant potential lower than the OCP (e.g., OCP = 0.23 V in 10 mM $NaNO_3$ solution) in principle overcomes this situation, or at least fixed the POT/POT^+ molar ratio in the membrane (with POT > > > > POT^+).

Subsequently, the application of an anodic linear sweep potential (for example from 0 to 1.2 V, step 2 in Fig. 1a) results in the gradual oxidation of POT to POT^+, which is stabilized by R^- with the concomitant release of Na^+ from the membrane to the solution. This generates the expected voltammetric peak.

Case 2. First addition of silver to the sample solution: After the application of the anodic linear sweep potential in the $NaNO_3$ solution (from 0 to 1.2 V), the potential of the system remains close to 1.2 V for a certain time. Therefore, POT is in its oxidized form while it is expected to spontaneously return to the neutral state over time. Then, if the reduction of POT^+ to POT is electrochemically forced by applying a constant potential (e.g., 0 V, considering OCP = 0.23 V) in the presence of Ag^+, its accumulation in the membrane may be realized. When a trace amount of Ag^+ is added to the solution, the reduction of POT^+ to POT is coupled to the entrance of both Na^+ and Ag^+ into the membrane during step 1 (Fig. 1b). Note that Ag^+ entrance is energetically favored by the presence of the ionophore (L) but it is still time-dependent due to the mass-transport control in the solution phase at very low concentrations of Ag^+.

As a result, two stripping peaks are expected during step 2 (see Fig. 1b). The first peak is associated with the Na^+ transfer and the second one with Ag^+ transfer. Because Ag^+ ion is binded to the ionophore,a higher Gibbs energy is therefore associated with this ion-transfer process [18,20]. The integrated charge, under the Na^+ peak, initially displayed for the background solution (case 1) is now divided between these two peaks because the total amount of the transferred charge across the membrane remains constant, as previously demonstrated [18].

Case 3. Increasing silver concentration in the sample solution: The Ag^+/Na^+ molar ratio entering the membrane depends on the amount of Ag^+ in the solution. As a result, increasing the Ag^+ concentration in the solution proves in more Ag^+ accumulation in the membrane during step 1, and therefore, the corresponding stripping peak is expected to increase while that for Na^+ decreases (Fig. 1c).

Fig. 2a presents the voltammograms at increasing concentrations of Ag^+ in 10 mM $NaNO_3$ by applying the proposed protocol (i.e., E_{app} = 0 V for t = 1440 s, stirring rate of 300 rpm, and linear sweep potential from 0 to 1.2 V at a scan rate of 100 mV s^{-1}). As expected, the voltammogram in the background electrolyte showed only one peak at 303 mV corresponding to Na^+ release to the solution (case 1). Notably, after the development of the stripping peak, the baseline did not reach its original value of close to zero µA and remains at ca 0.3 µA instead. This is a typical behavior already reported for thin voltammetry membranes based on ionophores, which displayed some charging currents in the range of 0.1–0.3 µA [18,21], but also for the thicker membranes reported by Amemiya et al., showing capacitive currents of 4 µA and even higher after the stripping peak [8]. Interestingly, despite no clear explanations having been reported in the literature for this change in the baseline, it seems to be a common behavior. In addition, increasing changes in the initial baseline were reported for increasing analyte concentration, scan rate, rotation speed of the electrode, and accumulation time as typical trends [8].

Once Ag^+ was added to the solution (from 5 to 100 nM), the peak for the Na^+ transfer gradually decreased until disappearing for Ag^+ concentration equal to 500 nM. This decrease of the Na^+ peak coincides with the appearance and increase of the peak corresponding to Ag^+ transfer from the membrane to the solution at 639–747 mV (depending on the Ag^+ concentration). As observed in Fig. 2a, once only one peak appeared for the Ag^+ transfer at 500 nM concentration in the solution, this peak did not increase any longer (see the peak for 1000 nM Ag^+ concentration in Fig. 2a) and, therefore, the saturation state of the membrane was reached. Indeed, the integrated charge under this peak (4.367 µC) was almost equal to that obtained for the sole Na^+ transfer (4.272 µC, 2% difference), noting that this charge is dictated by the amount of TFPB– (i.e., cation exchanger) initially present in the membrane as demonstrated in previous papers– [20].

Again here, there was a change in the baseline after the peak's development that increased with Ag^+ concentration in the solution. Furthermore, the peak width at half peak height ($W_{1/2}$) increased with the Ag^+ concentration, being close to 250 mV when only the peak of Ag^+ was present in the voltammogram. Note that, values for $W_{1/2}$ in the range of 210 mV have already been reported for thin membranes backside contacted with POT, as the oxidation/reduction of the POT film occurs through a process involving a number of electrons close to

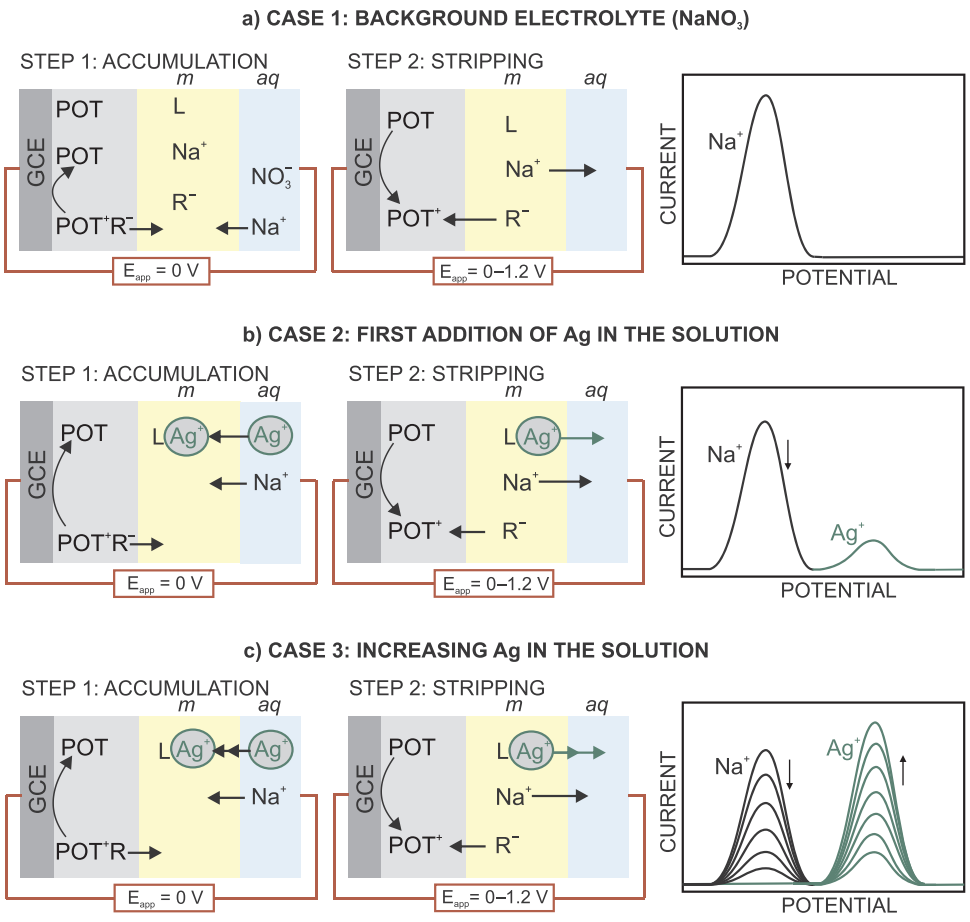

Fig. 1. Illustration of the working mechanism of the nanometer-sized membrane subjected at the established electrochemical protocol for accumulation and linear sweep stripping of silver at increasing concentrations in $NaNO_3$ background. GCE = glassy carbon electrode, m = membrane, aq = aqueous sample solution, Na^+R^- = cation exchanger NaTFPB, L = Ag ionophore.

0.5 [19].

Fig. 2b and c show the change in the peak current and charge for the Na^+ and Ag^+ transfer waves displayed in Fig. 2a. In addition, the total charge transferred across the membrane, calculated as the sum of the integrated charges under both peaks is presented in Fig. 2c (blue line). Note that the charge was integrated using a baseline correction followed by deconvolution and Gaussian fit of each peak as illustrated in Fig. S1.

Regarding the trend found for the peak current at increasing Ag^+ concentrations, it followed a linear relationship for both the Na^+ and the Ag^+ transfer from 5 nM up to 100 nM Ag^+ concentration, just before the saturation of the membrane. The same behavior was found for the integrated charge under the two peaks. It was also confirmed that the total amount of charge transferred across the membrane in the form of Na^+ plus Ag^+ transfer is maintained over the entire Ag^+ concentration range (with an average of 4.231 ± 0.151 μC, see blue line in Fig. 2c). Advantageously, the linearity found with the integrated charge revealed the potential of the developed electrode as a coulometry sensor, which may likely be very convenient toward the development of calibration-free sensors [5]. In both cases, peak current or charge selected as the analytical signal, the upper limit of the linear range of response corresponds to a Ag^+ concentration slightly lower than the one attributed to the membrane saturation (i.e., the linear range of response from 5 to 100 nM; saturation at 500 nM).

The necessity of the accumulation step in the established protocol was confirmed by several control experiments. First, the OCP of the electrode in a solution of 50 nM Ag^+ after the application of the entire accumulation/stripping protocol was registered over 2 h (Fig. S2). The OCP after the anodic potential scan (step 2) initially remains at a very positive potential (ca 0.85 V) and decreases abruptly during the first 10 s (from 856 to 585 mV, inset in Fig. S2) and then more slowly. This spontaneous decrease in the OCP indicates that the electrode is gradually returning to its initial state (OCP of 230 mV) by re-reduction of the oxidized POT^+ to POT. After two hours, the initial OCP is still not totally recovered (a total decrease of 578 mV was registered, from 585 to 278 mV, during this time), therefore justifying the use of the accumulation step in the developed protocol.

So that, in the accumulation step, the application of a constant potential to assure that POT is mainly in its neutral form is mandatory to provide Ag^+ accumulation into the membrane. Then, it is here anticipated that the time needed to reach the effective accumulation of Ag^+ into the membrane is mass-transport dependent, as demonstrated in the next section. Indeed, any spontaneous entrance of Ag^+ in the membrane at zero current conditions was evaluated by registering the electrode potential at increasing concentrations of Ag^+ in the solution (i.e., regular potentiometry experiment). A total increase of 20 mV was displayed in the range of 5 nM to 1 μM, meaning no response of the membrane at this concentration range.

3.2. Evaluation of the stripping peak of silver at different experimental conditions

Subsequently, the influence of all the parameters involved in the proposed protocol for Ag^+ stripping using nanometer-sized membranes was evaluated. The stirring rate was first varied (100–600 rpm, trying to avoid a very strong agitation speed that may damage such a thin membrane) during the accumulation step. As expected, because the membrane is under diffusional controlled mode, a certain level of stirring is necessary to assure that the Ag^+ present in the solution is effectively accumulated into the membrane at the established experimental conditions. Thus, for 500 nM Ag^+ concentration in the sample solution (Fig. 3a), when the stirring rate during the accumulation step

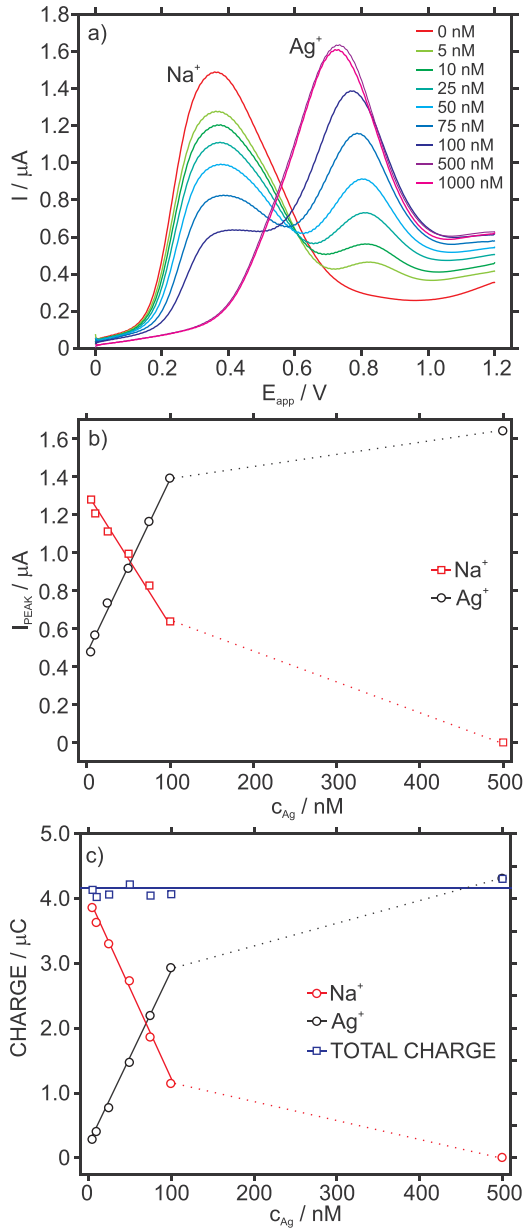

Fig. 2. (a) Linear sweep voltammograms observed during the stripping of Ag^+ at increasing concentrations (0, 5, 10, 25, 50, 75, 100, 500 and 1000 nM) in 10 mM $NaNO_3$ background solution. (b) Plot of the peak current for the peaks corresponding to the Na^+ and Ag^+ transfers versus the Ag^+ concentration. (c) Plot of the peak charge corresponding to the Na^+ and Ag^+ transfers as well as the sum of both versus the Ag^+ concentration. Applied protocol: E_{app} = 0 V during t = 1440 s, stirring speed of 300 rpm, scan rate of 100 mV s^{-1} and linear sweep potential from 0 to 1.2 V, with OCP^0 close to 230 mV.

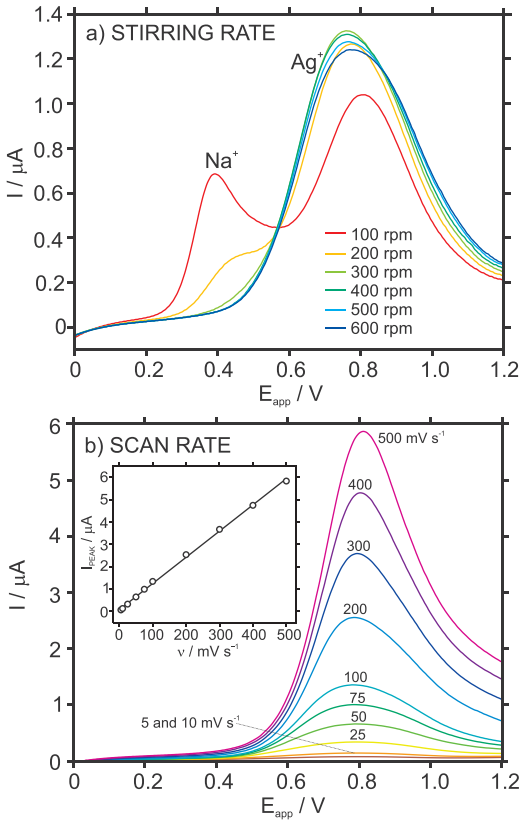

Fig. 3. (a) Linear sweep voltammograms observed during the stripping of 500 nM Ag^+ in 10 mM $NaNO_3$ background solution at increasing stirring speeds (100–600 rpm, trying to avoid a very strong stirring that may damage the membrane). Applied protocol: E_{app} = 0 V during t = 720 s, scan rate of 100 mV s^{-1} and linear sweep potential from 0 to 1.2 V. (b) Linear sweep voltammograms observed during the stripping of 500 nM Ag^+ in 10 mM $NaNO_3$ background solution at increasing scan rates (5–500 mV s^{-1}). Applied protocol: E_{app} = 0 V during t = 720 s, stirring speed of 300 rpm and linear sweep potential from 0 to 1.2 V. Notably, the accumulation time was reduced compared with the protocol used to perform the experiments shown in Fig. 2 to reduce the analysis time while studying the effect of the stirring speed and the scan rate at the saturation conditions of the membrane.

was in the range of 100–200 rpm, two peaks (for Na^+ and Ag^+) were observed in the voltammogram corresponding to the linear sweep stripping. In contrast, only the peak for Ag^+ transfer appeared at 300 rpm. This peak is then constant even if the speed is increased even more (up to 600 rpm). It is worth mentioning that to ensure the lowest limit of detection of the membrane electrode, it is convenient that the saturation of the electrode is produced at a very low Ag^+ concentration (such as 500 nM or even lower) to lower the limit of detection of the electrode.

Fig. 3b presents the voltammograms observed at increasing scan rates during the stripping step. A linear relationship was observed between the peak current and the scan rate, as expected in traditional stripping voltammetry [22]. In addition, when the scan rate was increased, the peak became narrower (for example $W_{1/2}$ was 370 mV at 100 mV s^{-1} and 250 at 500 mV s^{-1}), and this was accompanied by a gradual increase of the current baseline after the peak development, a trend that was previously reported by Amemiya et al. for Ca^{2+} detection [8].

The effect of the accumulation time on the stripping voltammograms was evaluated at two different concentrations of Ag^+: 500 nM (at which the membrane is saturated) and 5 nM (the lowest concentration displaying a peak for the Ag^+ transfer in the experiment shown in Fig. 2a). Fig. 4 depicts the observed voltammograms. Evidently, it is necessary to apply the accumulation potential for a certain time (720 s at the established experimental conditions), to generate saturation of the membrane at 500 nM of Ag^+ (Fig. 4a) or visualize the peak at very low concentration of Ag^+ (Fig. 4b). Conveniently, this long time may be reduced if the stirring rate during the accumulation step is increased. Indeed, these two parameters are crucial for the optimum limit of detection in a reasonable analysis time.

In this direction, we combined a long accumulation time of 2880 s with different stirring speeds to achieve the detection of 1 nM Ag (Fig. 5). Indeed, the stripping peak for 1 nM Ag was visualized when using 800 rpm during the accumulation step. However, the completion of the entire calibration graph at an accumulation time of 2880 s would take such a long time that the developed methodology would not be

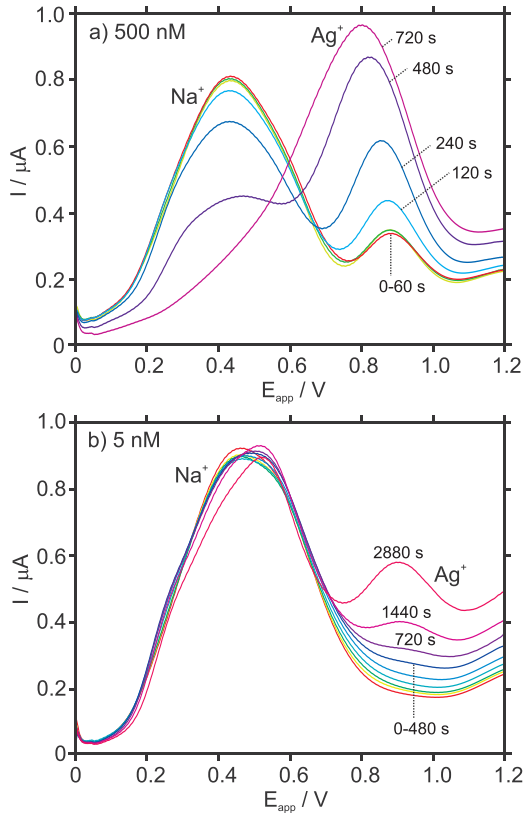

Fig. 4. (a) Linear sweep voltammograms observed during the stripping of 500 nM Ag^+ in 10 mM $NaNO_3$ background solution at increasing accumulation time (0, 20, 40, 60, 120, 240, 480, 720, and 960 s). Applied protocol: E_{app} = 0 V, stirring speed of 300 rpm, scan rate of 100 mV s^{-1} and linear sweep potential from 0 to 1.2 V. (b) Linear sweep voltammograms observed during the stripping of 5 nM Ag^+ in 10 mM $NaNO_3$ background solution at increasing accumulation time (0, 20, 40, 60, 120, 240, 480, 720, 1440, and 2880 s). Applied protocol: E_{app} = 0 V, stirring speed of 300 rpm, scan rate of 100 mV s^{-1} and linear sweep potential from 0 to 1.2 V.

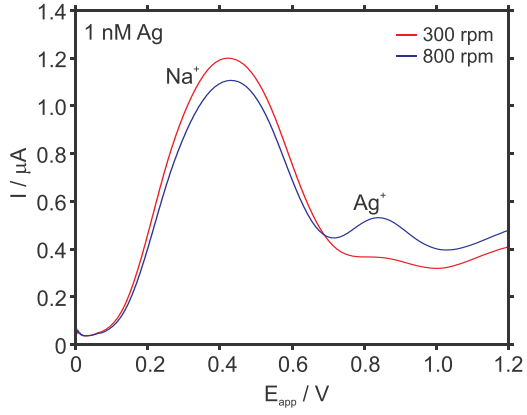

Fig. 5. Stripping voltammograms of 1 nM Ag^+ in 10 mM $NaNO_3$ background solution at 300 rpm and 800 rpm stirring speed. E_{app} = 0 V during 2880 s, linear sweep stripping from 0 to 1.2 V, scan rate of 100 mV s^{-1}.

suitable in terms of analysis time (practically, close to 50 min to analyze each sample).

The need for a long time to reach the effective accumulation of Ag^+ in the membrane pointed out several features of the working mechanism of the membrane. First, for a very low concentration of Ag^+ in the solution (such as 5 nM), while the Na^+ peak is displayed whatever the accumulation time was, a minimum of 720 s was needed to observe the Ag^+ peak (see Fig. 4b) and, indeed greater peak was displayed for such a long time as 2880 s (48 min). So that, considering that the re-reduction of POT^+ to POT at E_{app} = 0 V is a fast process, the long time needed for an effective Ag^+ accumulation into the membrane is given by its mass transport at the membrane-sample interface, its gradient across the membrane and the complexation with the ionophore (finally replacing the Na^+ that initially pairs the $TFPB^-$ from the undoping of POT at 0 V). The lower the Ag^+ concentration in the solution, the lower the mass transport in the solution, the lower its gradient across the membrane and therefore, the longer the time required for an effective accumulation in the membrane. As a result, while the application of the accumulation potential solves the long time needed for the spontaneous re-reduction of POT^+ to POT (see Fig. S2) while fixing exactly the same state of the POT film for each experiment, a long time is needed to accumulate the Ag^+ at such low concentrations. This latter is therefore the limiting step for the required analysis time.

It is now evident that the nanometer-sized membrane works on the basis of ion-exchange processes at the membrane-sample interface in both the accumulation and stripping steps. For the accumulation step, the presence of the silver ionophore influences the Na^+/Ag^+ ratio present in the membrane to compensate the negative charge of the $TFPB^-$ after POT undoping, as above mentioned. Thus, in an ideal case and considering that the reported selectivity coefficient for the ionophore is $logK^{pot}_{Na,Ag} = -7.4$ [23], in the presence of 10 mM Na^+ concentration (background solution in our experiments) it is expected that from a 50 nM Ag^+ concentration the membrane will preferentially show silver exchange. For lower concentrations, both Na^+ and Ag^+ ions will be exchanged. In our experiments, we exclusively found the Ag^+ peak at 500 nM concentration (what we referred as saturation of the electrode) at the established experimental conditions. This is indeed a close approximation to the ideal case.

Strictly speaking, the theoretical definition of both the accumulation and the stripping processes occurring at the membrane-sample interface is given by a Nernst-type equation for the activities of silver and sodium. Indeed, this is supported by previous observations of Amemiya group and our owns [7,8,17,18]. Notably, activity is equal to concentration in all our experiments owing to the very low amount of Ag^+ ions and the fixed ionic strength by the $NaNO_3$ background solution. Accordingly, calibration graphs are herein presented for increasing Ag^+ concentrations in the sample solution.

The dependence of the peak current (i_{peak}) generated under exhaustive analyte stripping from a thin membrane is well-known to be dependent on the analyte concentration in the membrane, which in turn depends on the preconcentration time, according to the following equation: [24]

$$i_{peak} = \frac{z^2 F^2 \upsilon V_m c_m(t_p)}{4 R T} \quad (1)$$

where υ is the potential sweep rate during the stripping process, V_m is the membrane volume, and $c_m(t_p)$ is the membrane ion concentration at the preconcentration time of t_p. On the basis of Eq. (1), Amemiya et al. developed one equation to define the limiting current (i_l) shown by the membrane at saturation conditions with the aim of justifying the long times required for effective accumulation of ions in thin membranes based on ionophores and subjected to potentiostatic transfer, as shown in Eq. (2) [8].

$$c_m(t_p) = \frac{i_l t_p}{z F V_m} \quad (2)$$

When this equation is applied to the Ag^+-selective membrane used in the present paper, the estimated t_p to reach the membrane saturation is 1057 s. This was calculated by considering $c_m(t_p)$ of 40 mmol L^{-1} (that is equal to the $TFPB^-$ concentration in the membrane at saturation conditions, i.e., exhaustive stripping of the analyte), i_l of 1.65 × 10^{-6} A (that is the experimental current observed for the peak corresponding to 500 nM Ag^+ concentration in Fig. 2a) and V_m of 4.57 × 10^{-7} L (5 mm of

diameter and 230 nm of thickness). Considering that the accumulation step is accomplished under stirring conditions, the time of 720 s for the saturation of the membrane to be achieved at 500 nM rather agrees with the calculation from this equation. Indeed, Amemiya et al. observed the need for accumulation times ranging from 30 to 60 min for the detection of Ca^{2+} [8] and even longer times for K^+ [7].

The magnitude of the applied potential in the accumulation step was also varied (Fig. S3). In principle, it is not expected that the applied potential has any influence in the observed stripping voltammograms for Ag^+ as long as its value is low enough to allow for a constant POT^+ reduction to its neutral form with the concomitant accumulation of Ag in the membrane. Effectively, similar stripping peaks for Ag were displayed (Fig. S3). Taking into account the voltammograms reported by Cuartero et al. for bare POT electrodes in organic solution, POT is present in its neutral form in a potential window from 0 to 0.5 V against the same Ag/AgCl reference electrode used throughout [19]. Note that this potential window lies just before the development of the stripping peak for Ag^+ as shown in Fig. 2a.

In this sense, the voltammograms at increasing Ag concentrations were rather similar without any dependence of the applied potential within the mentioned range (E_{app} from 0 to 0.5 V, see Fig. S3 for an illustration of the Ag^+ voltammetric peak), thereby presenting the same linear range of response for both the peak current and integrated charge as well as comparable sensitivity. As an example, the calibration curves observed with three twin electrodes that have been subjected to a protocol based on an applied potential of 0.22 V (instead of 0 V as displayed in Fig. 2) are shown in Fig. 6. Furthermore, the electrodes presented an excellent between-electrode reproducibility. It is hereby demonstrated that, owing to the interrogation of the membrane with the new electrochemical (accumulation/stripping) protocol, it is possible to detect nM levels of Ag^+ using nanometer-sized membranes, i.e., 1000-fold lower Ag^+ than employing regular cyclic voltammetry [18].

3.3. Detection of silver in water from different sources

In view of the very low concentration of Ag^+ detectable by the developed sensor (i.e., 5 nM), we analyzed the Ag^+ content of samples based on different matrices (10 mM $NaNO_3$ background, tap and lake water) by using the standard addition method. All the analyzed samples were previously characterized by ICP-MS (as described in the Supporting Information) and the results are listed in Table 1. Importantly, the Ag^+ contents in the tap and lake waters were 0.32 and 0.60 nM, respectively, according to the ICP-MS, i.e., more than 10 times lower than the linear range of response of the developed sensor.

In the absence of other kinds of samples with a higher Ag^+ content, the tap and lake water samples were spiked with known amounts of Ag^+ and analyzed, as well as the samples with $NaNO_3$ background, using both techniques. The Ag^+ content in all the $NaNO_3$ samples was really close to the added one, with recoveries ranging from ca 88 to 107%. Interestingly, there was no difference between using the peak current or charge to calculate the Ag^+ concentration compared with the values displayed by ICP-MS, confirming the appropriate baseline correction in the data treatment for the peaks' integration.

Fig. 7a shows the stripping voltammograms for increasing Ag^+ concentrations in tap water. It is worth mentioning that in the voltammogram corresponding to the non-spiked tap water (red line), three peaks are observed at ca 240, 600, and 750 mV. The entire charge transfer across the membrane appears as a broad band from 0 to 1.0 V (close to the entire potential window during the linear sweep voltammetry), as a result of the overlap of these three peaks. This unusual shape of the voltammogram indicates a certain matrix effect of the tap water on the electrode response, considering the variety of cations present in this sample.

Most probably, the peak at 240 mV mainly shows Na^+ transfer together with other cations with similar transfer energy. When Ag^+ was gradually added to the tap water, this peak decreased showing a similar trend as the Na^+ peak in $NaNO_3$ background solution, apart from the same peak position. Then, the peak at 600 mV slightly decreased when 10 nM Ag^+ was added to the solution and was almost negligible with 50 nM Ag^+. Because it disappeared before the peak at 240 mV (i.e. in the presence of a lower Ag^+ concentration), this indicates that the concentration of the cation showing the peak at 600 mV is lower than the Na^+ concentration in the tap water. In addition, because the peak position is closer to the Ag^+ peak (the one at 750 mV) than that for Na^+

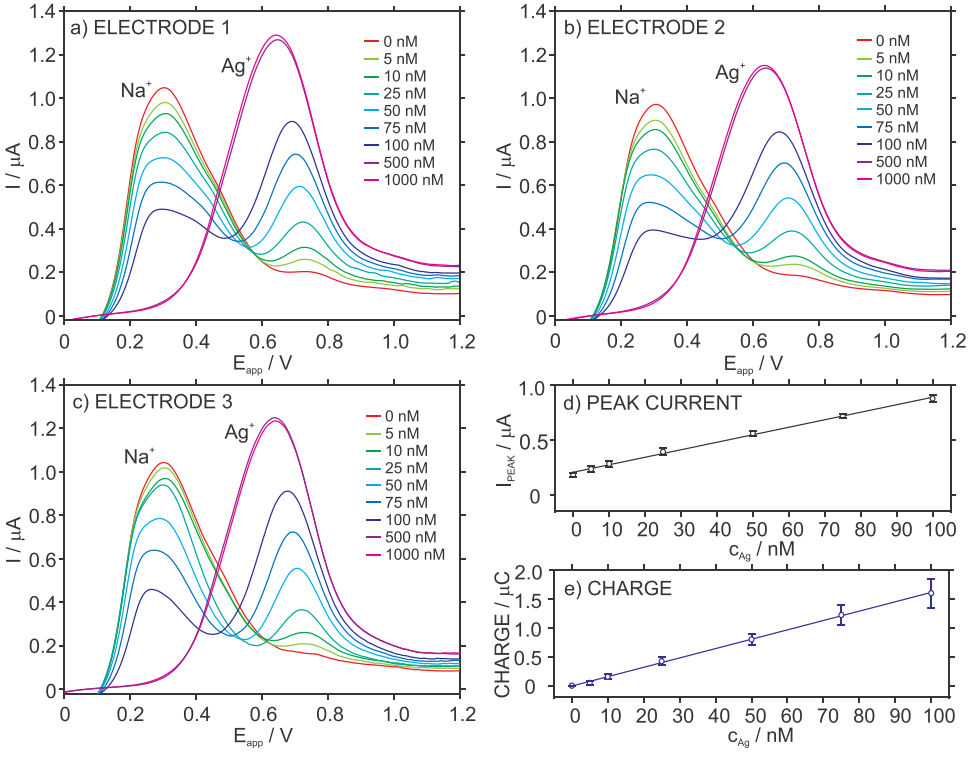

Fig. 6. Stripping voltammograms observed at increasing concentrations of Ag using three twin electrodes (a–c). Corresponding calibration curves using the peak current (d) and the integrated charge (e) corresponding to the Ag^+ transfer as the analytical signal. E_{app} = 0.22 V during 720 s, stirring speed of 300 rpm, linear sweep stripping from 0 to 1.2 V, scan rate of 100 mV s^{-1}.

Table 1
Silver detection in artificial and real samples.

Matrix	Ag^+ (nM)	Electrode						ICP-MS			% Difference (Electrode *vs* ICP-MS)	
		I_{peak}			charge			c_{Ag} (nM)	RSD	% Recovery	I_{peak}	charge
		c_{Ag} (nM)	RSD	% Recovery	c_{Ag} (nM)	RSD	% recovery					
10 mM $NaNO_3$	10	9.69	0.04	96.9	10.18	0.29	101.8	10.26	1.03	102.6	5	0.8
	50	50.30	0.01	100.6	43.92	0.79	87.8	53.61	1.07	107.2	6	18
	100	–	–	–	–	–	–	106.25	0.90	106.3	–	–
	500	–	–	–	–	–	–	505.69	0.73	101.1	–	–
Tap water	0	–	–	–	–	–	–	0.32	5.4	–	–	–
	10	15.41	0.01	154.0	7.62	0.38	76.2	9.30	0.87	93.0	> 50	18
	50	50.26	0.04	100.5	58.42	0.11	116.8	43.80	1.29	87.6	14	33
Lake water	0	–	–	–	–	–	–	0.60	4.9	–	–	–
	10	16.75	0.33	167.5	–	–	–	5.46	3.4	54.6	> 50	–
	50	43.33	0.18	86.6	–	–	–	31.62	2.23	63.2	37	–

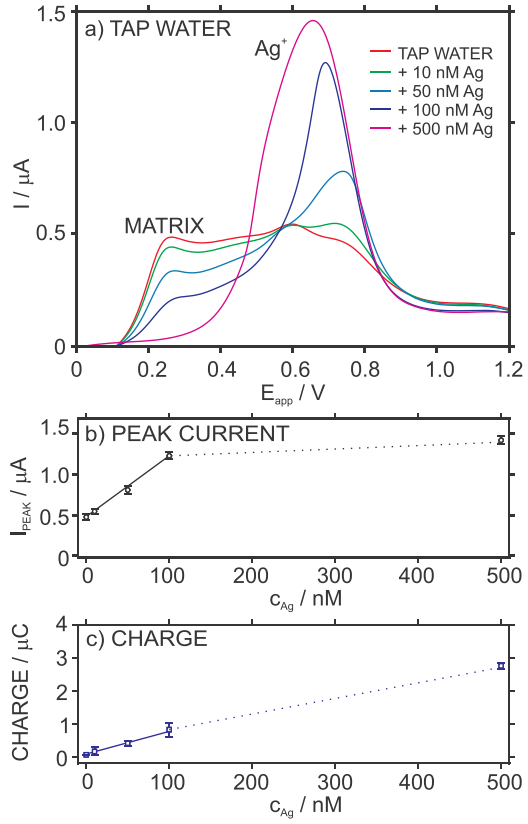

Fig. 7. (a) Stripping voltammograms observed at increasing concentrations of silver in tap water matrix. (b) Plot of the peak current corresponding to Ag^+ transfer versus Ag^+ concentration in the sample. (c) Plot of the integrated charge under peak corresponding to the Ag^+ transfer versus Ag^+ concentration in the sample. E_{app} = 0.22 V during 720 s, stirring speed of 300 rpm, linear sweep stripping from 0 to 1.2 V, scan rate of 100 mV s^{-1}.

(250 mV), this points out that the peak at 600 mV corresponds to a cation for which the ionophore is more selective than for Na^+. This conclusion is supported by our previous results demonstrating that the peak position for one cation transfer in voltammetry thin membranes based on a selective ionophore depends on the binding constant [20]. According to these two conclusions, the peak at 600 mV likely corresponds to other trace cation (most likely a metal) present in the sample at trace concentrations. But to be more precise, separate experiments with other cations have to be accomplished to identify this peak, which is not herein necessary for practical purposes.

Regarding the last peak at 750 mV, the peak position is within the potential range for the Ag^+ transfer displayed in $NaNO_3$ background solution (see Figs. 2a and 6 a–c for comparison), and then this peak is the only that increased with the Ag^+ concentration in the sample solution. As a result, this peak was ascribed to the presence of Ag^+ in the sample.'

In relation to this, Fig. 7b and c presents the plots of the peak current and the integrated charge *versus* the silver concentration in the tap water, respectively. The Ag^+ concentration range for the linear response of the electrode starts at a slightly higher Ag^+ concentration than that observed in $NaNO_3$ background (10–100 nM against 5–100 nM), probably due to the mentioned matrix effect. Good reproducibility of these results was observed using different electrodes, as shown by the error bars in Fig. 7b and c corresponding to the three calibrations presented in Fig. S4.

Fig. 8a depicts the stripping voltammograms for increasing Ag^+ concentrations in the lake water sample. Analogous to the tap water, several peaks appeared in the non-spiked sample and the Ag^+ peak is identified at ca 750 mV. However, in this case, the peak slightly increased in the concentration range from 5 to 100 nM, and then abruptly

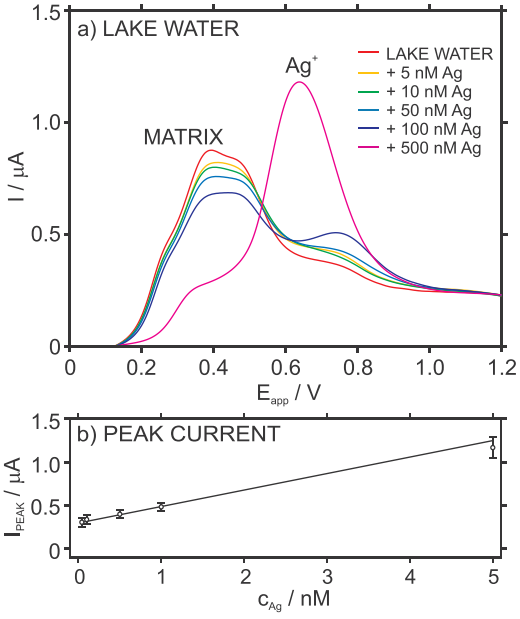

Fig. 8. (a) Stripping voltammograms observed at increasing concentrations of silver in lake water matrix. (b) Plot of the peak current corresponding to Ag^+ transfer versus Ag^+ concentration in the sample. E_{app} = 0.22 V during 720 s, stirring speed of 300 rpm, linear sweep stripping from 0 to 1.2 V, scan rate of 100 mV s^{-1}.

increased up to the saturation state at 500 nM. Indeed, this behavior is reproducible for different electrodes (Fig. S5) and when intermediate concentrations are tested between 100 and 500 nM, the saturation state is always reached after 100 nM (data not shown). As a result, the peak current may be followed as the analytical signal (indeed it shows linearity from 5 to 100 nM, see Fig. 8b), but the error associated with charge integration is such with these small peaks that we could not find any linear relationship with the Ag^+ concentration in the sample (see Fig. S6).

Silver detection was finally demonstrated in tap water and lake water using the standard addition method. As observed in Table 1, the results obtained with the developed electrode showed rather good percentage recoveries, whereas Ag^+ content was always underestimated using ICP-MS, especially in the case of lake water samples. We are not the first to find this kind of underestimation using ICP-MS when analyzing environmental waters (such as seawater or others), and it is normally associated with a matrix effect occasioned by the large number of other ions in the sample in comparison with the traces of Ag [25,26]. Overall, as the complexity of the sample increases, the differences between the results obtained by our method and those obtained using ICP-MS increased (see Table 1). In addition, the samples measured by ICP-MS were previously filtered, while they were measured as sampled by the developed electrode.

4. Conclusions

Nanometer-sized membranes based on silver ionophore and backside contacted with POT have demonstrated herein the capability of measuring nanomolar levels of silver in real complex matrix by changing the interrogation protocol to an accumulation/stripping electrochemical method rather than traditional cyclic voltammetry. After the application of an anodic linear sweep potential scan, the POT film mainly remains in its oxidized form and is forced to return to its neutral state with the switching to a constant potential of 0 V over a certain period of time. Connected to this process of POT re-reduction, silver ions present in the solution enter the membrane to fulfill the electroneutrality requirements, and, consequently, there is a controlled enrichment of silver in the membrane. This produces the voltammetric peak associated with the release of silver during a subsequent anodic linear sweep potential scan, which is visible from a 1 nM silver concentration (a thousand-times-lower concentration than that when the membrane is interrogated by cyclic voltammetry). Thus, silver detection is possible in environmental waters with a silver content from 5 to 100 nM. Further work will be dedicated to reducing even more the limit of detection of nanometer-sized membranes pursuing trace metal detection in all kinds of natural waters.

Acknowledgments

The authors acknowledge the financial support of KTH Royal Institute of Technology (Starting Grant Programme K-2017-0371) and the Swedish Research Council (Project Grant VR-2017-4887). M.C. acknowledges the European Union (Marie Skłodowska-Curie Individual Fellowship, H2020-MSCA-IF-2017, Grant no. 792824). K.X. gratefully thanks the China Scholarship Council for supporting his Ph.D. studies. Special thanks to Alex Wiorek for support with the codes used for the data treatment and Prof. Lyubchenko for help in the preparation of the holders for the electrode modification. We are very grateful to Miguel Coll for the support in the characterization of water samples using ICP-MS.

Appendix A. Supplementary data

Supplementary material related to this article can be found, in the online version, at doi:https://doi.org/10.1016/j.snb.2019.126781.

References

[1] E. Zdrachek, E. Bakker, Potentiometric sensing, Anal. Chem. 91 (2019) 2–26.
[2] M. Cuartero, G.A. Crespo, All-solid-state potentiometric sensors: a new wave for in situ aquatic research, Curr. Opin. Electrochem. 10 (2018) 98–106.
[3] G.A. Crespo, E. Bakker, Dynamic electrochemistry with ionophore based ion-selective membranes, RSC Adv. 3 (2013) 25461–25474.
[4] M. Cuartero, G.A. Crespo, E. Bakker, Thin layer samples controlled by dynamic electrochemistry, Chimia 69 (2015) 203–206.
[5] E. Bakker, Can calibration-free sensors be realized? ACS Sens. 1 (2016) 838–841.
[6] J. Bobacka, A. Ivaska, A. Lewenstam, Potentiometric ion sensors, Chem. Rev. 108 (2008) 329–351.
[7] B. Kabagambe, A. Izadyar, S. Amemiya, Stripping voltammetry of nanomolar potassium and ammonium ions using a valinomycin-doped double-polymer electrode, Anal. Chem. 84 (2012) 7979–7986.
[8] B. Kabagambe, M.B. Garada, R. Ishimatsu, S. Amemiya, Subnanomolar detection limit of stripping voltammetric Ca2+-selective electrode: effects of analyte charge and sample contamination, Anal. Chem. 86 (2014) 7939–7946.
[9] J. Zhang, A.R. Harris, R.W. Cattrall, A.M. Bond, Voltammetric ion-selective electrodes for the selective determination of cations and anions, Anal. Chem. 82 (2010) 1624–1633.
[10] A.R. Harris, J. Zhang, R.W. Cattrall, A.M. Bond, Applications of voltammetric ion selective electrodes to complex matrices, Anal. Meth. U. K. 5 (2013) 3840–3852.
[11] M. Cuartero, R.G. Acres, J. Bradley, Z. Jarolimova, L. Wang, E. Bakker, G.A. Crespo, R. De Marco, Electrochemical mechanism of ferrocene-based redox molecules in thin film membrane electrodes, Electrochim. Acta 238 (2017) 357–367.
[12] M. Sohail, R. De Marco, Z. Jarolimova, M. Pawlak, E. Bakker, N. He, R.M. Latonen, T. Lindfors, J. Bobacka, Transportation and accumulation of redox active species at the buried interfaces of plasticized membrane electrodes, Langmuir 31 (2015) 10599–10609.
[13] S. Jansod, L. Wang, M. Cuartero, E. Bakker, Electrochemical ion transfer mediated by a lipophilic Os(II)/Os(III) dinonyl bipyridyl probe incorporated in thin film membranes, Chem. Commun. 53 (2017) 10757–10760.
[14] Z. Jarolimova, J. Bosson, G.M. Labrador, J. Lacour, E. Bakker, Ion transfer voltammetry at thin films based on functionalized cationic 6 helicenes, Electroanal 30 (2018) 650–657.
[15] Z. Jarolimova, J. Bosson, G.M. Labrador, J. Lacour, E. Bakker, Ion transfer voltammetry in polyurethane thin films based on functionalised cationic 6 helicenes for carbonate detection, Electroanalytical 30 (2018) 1378–1385.
[16] P.C. Si, E. Bakker, Thin layer electrochemical extraction of non-redoxactive cations with an anion-exchanging conducting polymer overlaid with a selective membrane, Chem. Commun. (2009) 5260–5262.
[17] G.A. Crespo, M. Cuartero, E. Bakker, Thin layer ionophore-based membrane for multianalyte ion activity detection, Anal. Chem. 87 (2015) 7729–7737.
[18] D.J. Yuan, M. Cuartero, G.A. Crespo, E. Bakker, Voltammetric thin-layer lonophore-based films: part 1. Experimental evidence and numerical simulations, Anal. Chem. 89 (2017) 586–594.
[19] M. Cuartero, R.G. Acres, R. De Marco, E. Bakker, G.A. Crespo, Electrochemical ion transfer with thin films of poly(3-octylthiophene), Anal. Chem. 88 (2016) 6939–6946.
[20] M. Cuartero, G.A. Crespo, E. Bakker, Ionophore-based voltammetric ion activity sensing with thin layer membranes, Anal. Chem. 88 (2016) 1654–1660.
[21] M. Cuartero, G.A. Crespo, E. Bakker, Polyurethane ionophore-based thin layer membranes for voltammetric ion activity sensing, Anal. Chem. 88 (2016) 5649–5654.
[22] P.N. Bartlett, G. Denuault, M.F.B. Sousa, A study of the preconcentration and stripping voltammetry of Pb(II) at carbon electrodes, Analyst 125 (2000) 1135–1138.
[23] A. Ceresa, A. Radu, S. Peper, E. Bakker, E. Pretsch, Rational design of potentiometric trace level ion sensors. A Ag+-selective electrode with a 100 ppt detection limit, Anal. Chem. 74 (2002) 4027–4036.
[24] A.J. Bard, L.R. Faulkner, Electrochemical Methods: Fundaments and Applications, John Wiley & Sons, New York, 2001.
[25] F. Valverde, M. Costas, F. Pena, I. Lavilla, C. Bendicho, Determination of total silver and silver species in coastal seawater by inductively-coupled plasma mass spectrometry after batch sorption experiments with Chelex-100 resin, Chem. Spec. Bioavail. 20 (2008) 217–226.
[26] Z.H. Zhu, A.R. Zheng, Automated flow injection coupled with ICP-MS for the online determination of trace silver in seawater, Spectroscopy-US 32 (2017) 50–59.

Kequan Xu was Born in Xilinhot, Inner Mongolia (China). He received his BSc in Polymer Science and Engineering in 2013 at the Beijing University of Chemical Technology (China). Then, Kequan Xu moved to Royal Institute of Technology (KTH) in Stockholm (Sweden), where he obtained his MSc in Materials Science and Engineering in 2016. He is currently developing the PhD at KTH under the supervision of Gaston A. Crespo and Maria Cuartero. Kequan Xu is interesting in the development of electrochemical sensors with superior features for the detection of trace metals in environmental water samples.

Maria Cuartero was born in Murcia (Spain). She studied BSc in Chemistry and MSc in Advanced Chemistry at the University of Murcia (Spain). Maria Cuartero obtained her PhD degree in 2014 and then, she moved to the University of Geneva (Switzerland) for a postdoctoral stage in the group of Prof. Eric Bakker (2014–2017). Since 2018, Maria Cuartero is developing her scientific career at the Royal Institute of Technology (KTH) in Stockholm (Sweden), first as a Wenner-Gren fellow and now as Marie Curie fellow. Besides the development of her Marie Curie project (VolThinSens), Maria Cuartero is

involved in several research lines mainly comprising electrochemical sensors for environmental water analysis, enzymatic (bio)sensors, wearable sensors for healthcare and sport performance monitoring, spectroelectrochemistry and scanning-electrochemical microscopy. She is co-author of 60 peer-reviewed papers mainly in journals related to Analytical Chemistry and Electrochemistry fields.

Gaston A. Crespo born in Buenos Aires (Argentina), Gaston A. Crespo studied Chemistry at the University of Buenos Aires (UBA) where he received the Licentiate degree (1999–2005). He then moved to the University Rovira I Virgili at Tarragona (Spain), where he acquired a Master of Nanotechnology and Nanoscience and Doctoral degrees in 2007 and 2010, respectively. Thereafter, he joined Professor Eric Bakker's group at the University of Geneva (Switzerland) as a Postdoctoral Assistant (2011–2013) and in 2014, he was promoted to a Maître Assistant (comparable to Lecturer) at the same university. Since 2017, Gaston A. Crespo has held a tenure-track Assistant Professorship at the Royal Institute of Technology (KTH) located in Stockholm (Sweden). His research interests are in electroanalytical chemistry, membrane transport, development of electrochemical techniques, electrochemiluminiscence and optical sensors for environmental and biomedical applications, triggered devices and synchrotron characterization among others. He is co-author of > 90 peer reviewed publications, several patents and co-founder of spin-off companies.